Bitlis Eren Üniversitesi Fen Bilimleri Dergisi
BİTLİS EREN UNIVERSITY JOURNAL OF SCIENCE
ISSN: 2147-3129/e-ISSN: 2147-3188
VOLUME: 12 NO: 3 PAGE: 617-624 YEAR: 2023
DOI:10.17798/bitlisfen.1224055

# Design and Thermal Analysis of a Parabolic Collector

Cuma ÇETİNER[1*]

[1] *Harran University, Faculty of Engineering, Department of Mechanical Engineering, Şanlıurfa, Turkey*
*ORCID: 0000-0002-5105-5699*

**Keywords:** Solar energy, Parabolic collector, Thermal efficiency, Design collector

**Abstract**
In this study, the sun follow-up systematic parabolic collector typed collector's design and experimental study were made. The system provides sun tracking in the east-west direction. Instead of a mirror, chromium-nickel metal was used to reflect the sun's rays onto the focusing tube. Sanliurfa offers a conducive environment for conducting systematic performance evaluations through a series of thoughtfully designed experiments. These experiments aim to compare theoretical values with actual experimental results, ensuring a comprehensive analysis of the system's capabilities. It was possible to obtain 380 W of thermal power from the collector, whose area is 1.2 m$^2$. The thermal efficiency is high at 43% and low at 26%.

## 1. Introduction

The interest in continuous renewable energy sources is increasing, especially solar heating, cooling, and electricity generation are spreading. Solar concentrators are used to achieve high temperatures with solar radiation. They follow the sun on only one axis or two. There is a wide variety of solar collectors [1,2]. These are examined in two parts linear focus (Fresnel and parabolic collector type) and point (dish type and tower type) focus. The parabolic solar collector transfers the thermal energy to oil, water, and a similar flow by reflecting the sun rays with mirrors placed towards the absorber at the parabolic focal point on its surface and circulating it in the system. It is possible to reach very high temperatures using a very large parabolic surface area. Parabolic collectors work only with direct radiation and are more efficient in areas with plenty of sun throughout the year.

The flat reflector is used in Heliostat-type and Fresnel-type collectors. In the manufacture of dish-type and trough-type parabolic collectors, special manufacturing is required to use the mirror on the parabolic surface. In the manufacture of the parabola, easily shaped aluminum or chrome-nickel surface plate can be used to act as a reflector in terms of material. Venegas-Reyes designed a solar parabolic trough concentrator (PTC), 4.88 m high and 5.8 m$^2$ aperture area, with aluminum construction and efficiency of approximately 60% [3]. Irving Eleazar conducted a fascinating study on a parabolic field collector, measuring an impressive 2.44 m in length and 1.6 m in width, providing a collection area of approximately 3.8 m$^2$. The aluminum plate is used as reflective material in the parabolic collector whose construction is made of aluminum, and it is stated that its thermal efficiency is around 60% [4]. The thermal efficiency shows that the reflector, absorber material, environment, and heat carrier vary according to the fluid [5]. However, the efficiency of flat collectors is high (70%) [6].

In this study, chromium-nickel material was used as reflective material. This collector, which has 1.5 x 0.80 m dimensions and a 1.2 m$^2$ opening area, was circulated with a flow rate of 0.04 kg/s. The theoretical thermal efficiency of the system was compared with the experimental findings.

## 2. Material and Method

Figures 1 and 2 visually demonstrate the intriguing process where the sun's rays converge at the focal point, resulting in the transformation of the reflective material into a parabolic surface. The

*Corresponding author: ccetiner@harran.edu.tr
*Received: 25.12.2022, Accepted: 16.09.2023*

copper tube is placed inside the glass tube. The low-temperature water entering from $T_{in}$, shown in Figure 2, is collected in the tank, leaving the $T_{out}$ section. The water in the tank is re-entered into the pipe with a pump and the water in the system is circulated. With the current coming from the solar ray's sensor placed on the parabolic collector, the tracking system moves the collector toward the direction of the sun's rays. The parabolic collector has a solar sensor as shown in Figure 1 and follows the sun in the east-west direction. It follows the sun automatically with the electronic card as shown in Figure 2 in the control unit. The system acts according to the radiation detected in the sun sensor. In the experiments, the inlet and outlet temperatures of the water, the ambient temperature, and the glass temperature were measured with a data logger.

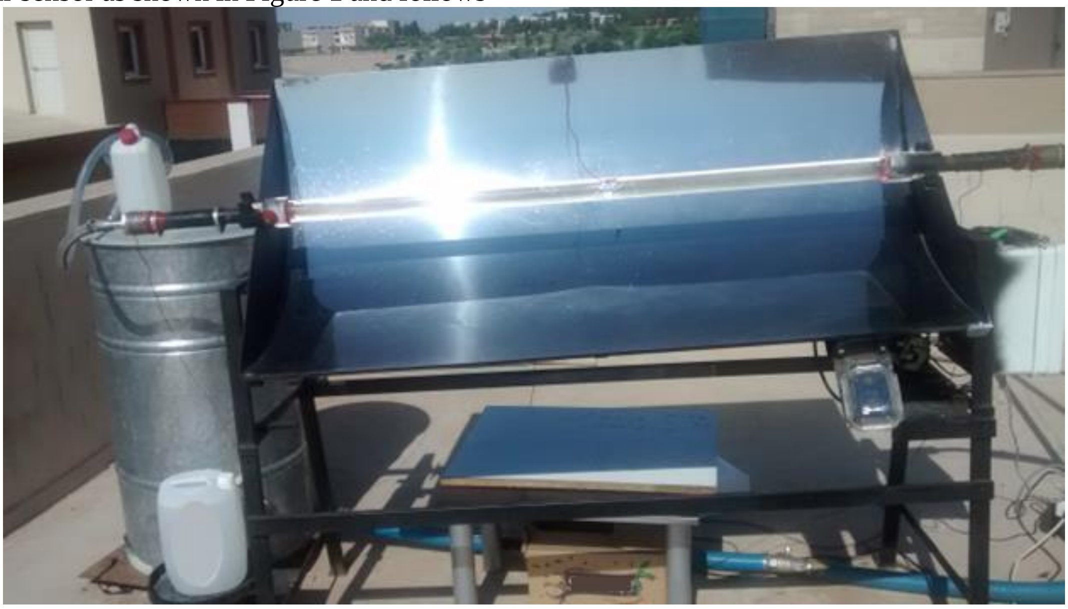

**Figure 1**. Inlet, outlet, glass, and ambient temperature measurements in the parabolic collector

As seen in Figure 2 and Figure 3, the length of the concentrator is 150 cm (L) with a parabolic opening of 80 cm (B). The copper outer diameter of the pipe used for the absorber is 35 mm and the inner diameter is 32 mm. A glass tube is placed inside this 42 mm diameter copper tube. The flow rate of the circulated water is 0.040 kg/sec.

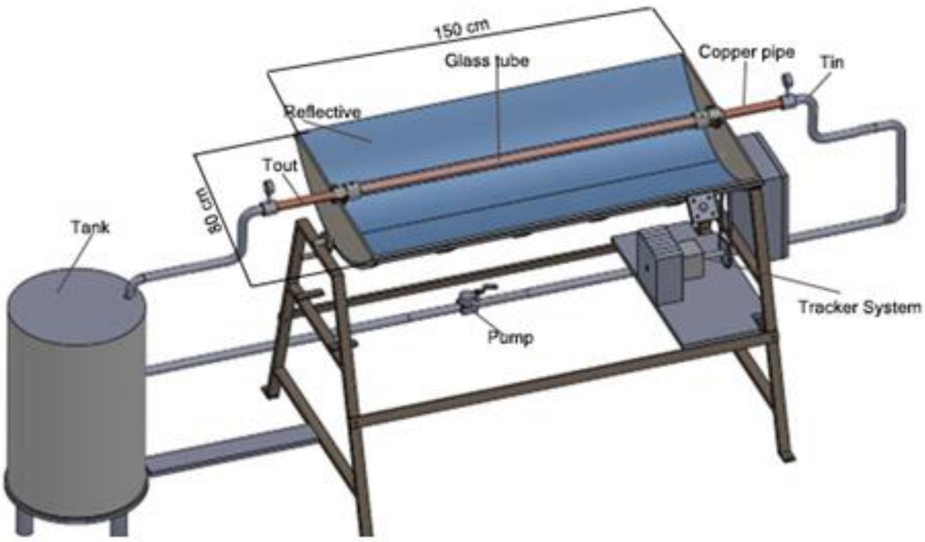


**Figure 2.** Parts of the parabolic collector

Equation (1) is related to the manufacture of the parabolic collector, f is the focal length (20 cm), y is the collector aperture (40 cm), x is the height (20 cm), and L is the length (150 cm). The x and y values obtained in Equation 1 for the parabolic collector designed for manufacturing are given in Table 1.

$$y = \sqrt{4\,f\,x} \tag{1}$$

**Table 1.** Parabolic of the collector coordinate values

| X(cm) | 20.0 | 15.8 | 12.1 | 8.9 | 6.2 | 4.0 | 2.2 | 1.0 |
|---|---|---|---|---|---|---|---|---|
| Y(cm) | -40.0 | -35.6 | -31.1 | -26.7 | -22.2 | -17.8 | -13.3 | -8.9 |

As seen in Figure 3 below, the x arm gives the height of the parabolic, and the 2y value gives the total span length of the parabolic. The focal length has been taken to be the same as the height for ease of fabrication.

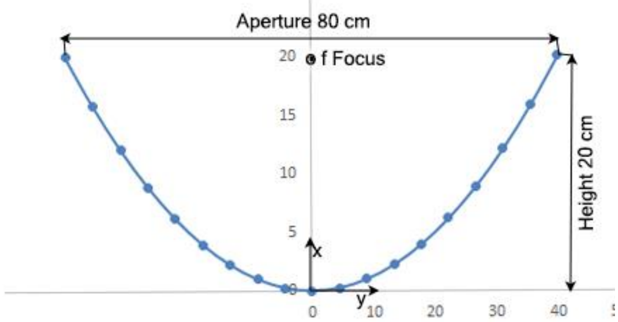


**Figure 3**. Height, width, and focal dimensions of the parabolic collector

## 3. Thermal Analysis of Parabolic Collector

While some of the amounts of radiation reaching the absorber from the condenser are thrown into the low-temperature environment due to losses, the other part is absorbed by the fluid and turns into useful energy. The useful thermal energy of the parabolic collectors transferred to the fluid in the absorber can be found in the following Hotel-Willer-Bliss equation 2 [7].

$$Q_u = A_a F_R \left[ I_d \alpha \rho \gamma \tau - \frac{A_y}{A_a} U_T (T_{in} - T_a) \right] \tag{2}$$

In this equation ($Q_u$) is the useful heat energy, ($A_a$) is the aperture area, ($A_y$) is the absorber area, ($F_R$) is the heat gain factor, and ($I_d$) represents the amount of direct radiation falling over the unit aperture area. α is the absorption rate of the absorber material, ρ is the reflectance rate of the reflective material, γ is the intercept factor, and τ is the transmittance coefficient of the transparent cover. ($U_T$) is the total heat transfer coefficient given from the absorber to the environment, ($T_{in}$) is indicated by the fluid inlet temperature and the ambient temperature ($T_a$).

The thermal efficiency of the concentrator and the useful thermal power of the collector are found by the aperture area of the parabolic collector and the rate of incident direct radiation. Accordingly, the theoretical thermal efficiency is as follows [7],

$$\eta_0 = \frac{Q_u}{A_a I_d} = F_R(\tau\alpha\gamma\tau) - F_R U_T \frac{A_y (T_{in} - T_a)}{A_a I_d} \tag{3}$$

In addition, when the inlet and temperatures of the fluid and the experimental values such as the flow rate are known, the thermal power can be found from the equation given below.

$$Q_u = m\, c_p (T_{out} - T_{in}) \tag{4}$$

Here, m is the flow rate and $T_{out}$ is the exit temperature of the fluid from the absorber. Thermal efficiency is defined as the ratio of the amount of heat transferred to the water to the direct solar energy coming to the total reflective surface. Accordingly, thermal efficiency is found equality as follows.

$$\eta = \frac{m\, c_p (T_{out} - T_{in})}{A_a I_d} \tag{5}$$

### 3.1 Calculation of Total Heat Transfer Coefficient

For the heat gains and losses in the parabolic collector, the total heat transfer coefficient in the pipe must be calculated. The total heat transfer coefficient $U_T$ for conduction, convection, and radiation heat losses from the absorber to the environment can be found in equation (6) below [8].

$$U_T = \left[ \frac{A_y}{A_a (h_{bc} + h_{rc})} + \frac{1}{h_w} \right]^{-1} \tag{6}$$

The losses occur by radiation and convection emitted from the outer surface of the absorber tube to the environment. As shown in the total heat transfer equation, it is necessary to calculate the radiation resistances in the pipe in terms of convection. Forced convection occurs on the outer surface of the glass pipe due to the wind in the environment. Reynold and Nusselt's values must be found because forced convective conditions occur. Nusselt value is suitable for glass pipe in the horizontal position (Equation 7) [9].

$$Nu = \frac{\rho VD_c}{\mu} = 0.193Re^{0.618}Pr^{0.333} \tag{7}$$

After the equation is found, the forced ($h_{bc}$) value is found. The radiation between the glass tube and the medium is shown in equation 8.

$$h_{rc} = \varepsilon_r\sigma(T_c + T_a)(T_c^2 + T_a^2) \tag{8}$$

The radiation coefficient occurs between the copper tube and the glass tube. Where Tc is the transparent cover temperature, Stefean-Boltzman constant, and εc is the radiation emission coefficient of the surface.

The radiation between the copper tube and the glass tube is the radiation between two parallel plates. It is found from the following equation 9 in terms of convection.

$$h_w = \frac{\sigma(T_c+T_a)(T_c^2+T_a^2)}{\frac{1}{\varepsilon_r}+\frac{A_r}{A_a}(\frac{1}{\varepsilon_c}-1)} \tag{9}$$

From equations 7, 8, and 9 above, the total heat loss coefficient for the absorber is found by substituting it in equation 6.

The heat gain factor $F_R$ for the collector used in the useful power equation is derived from the following equation 10 [10].

$$F_R = \frac{\dot{m}c_p}{A_rU_T}\left[1 - exp\left(-\frac{A_yU_TF}{\dot{m}c_p}\right)\right] \tag{10}$$

Here, the collector efficiency factor F is independent of the operating conditions and is a factor dependent on the construction of the collector. This value is found in the equation 11 below.

$$F = \frac{\frac{1}{U_T}}{\frac{1}{U_T}+\frac{d_d}{h_wd_i}+\frac{d_dln(\frac{d_d}{d_i})}{2k}} \tag{11}$$

When the values in equations 10 and 11 were put in their places, the heat gain factor $F_R$ was found to be 0.98. An Excel file was prepared to use the formulas given above and theoretical values were obtained.

## 4. Results and Discussion

The experiments were carried out in Şanlıurfa (e=37.1) between 8 a.m. and 5 p.m. In the collector, which is manufactured in small sizes, water is circulated at a low flow rate. Equation 3 was used for the theoretical thermal efficiency. In the calculation made, the total heat transfer coefficient from the glass pipe to the environment is around 4.98 W/m$^2$K. Since the copper pipe is not selective, the absorption ratio of the pipe is 0.82, the transmittance coefficient of the glass pipe is 0.83, and since the reflective surface is not a mirror, the reflection ratio is 0.75 and the intercept factor is 0.95. Using these values, the theoretical thermal efficiency value was calculated as 46-48% (Figure 4). Experimental efficiency was found from equation 5 by using inlet and outlet water temperatures and flow rates in the experiment. It can be seen in Figure 4 that the curve found for the experimental experiment is closer to the theoretical thermal efficiency in the afternoon.

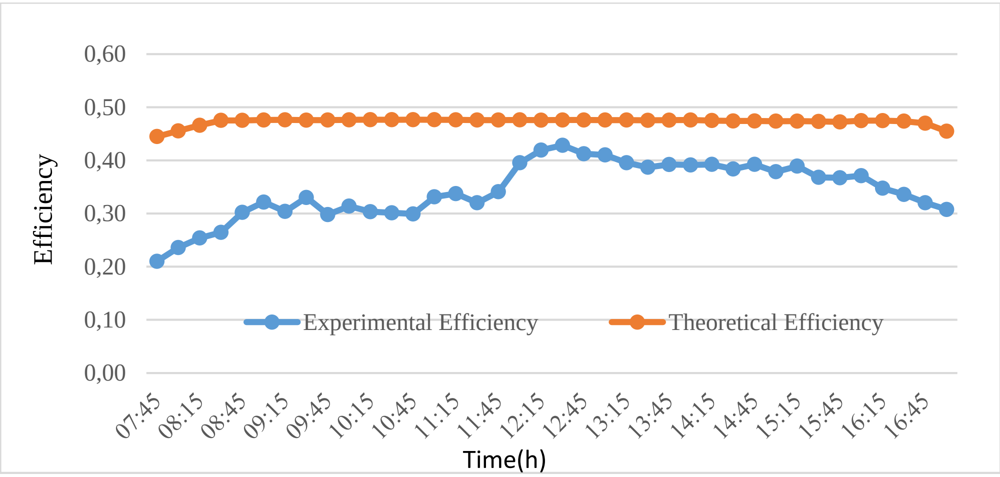


**Figure 4.** Theoretical and experimental thermal efficiency

The measured direct radiation value is around 600 to 800 W/m$^2$. Thermal efficiency calculations were made with direct radiation values (Sanliurfa, Lat 37.1). The radiation values were taken from the radiation measurement center at Harran University Engineering Faculty. The experimental section was set up at a distance of 20 m from this measurement center [11]. It was calculated that approximately 420 W of thermal power could be obtained theoretically from the parabolic collector (Figure 5). The reflectance rate, transmittance and absorption coefficient values selected in the theoretical calculation are effective. It is seen that the experimental results are closer to the useful power value at noon. In the morning and evening times, the thermal power values also decrease due to the low solar radiation intensity.

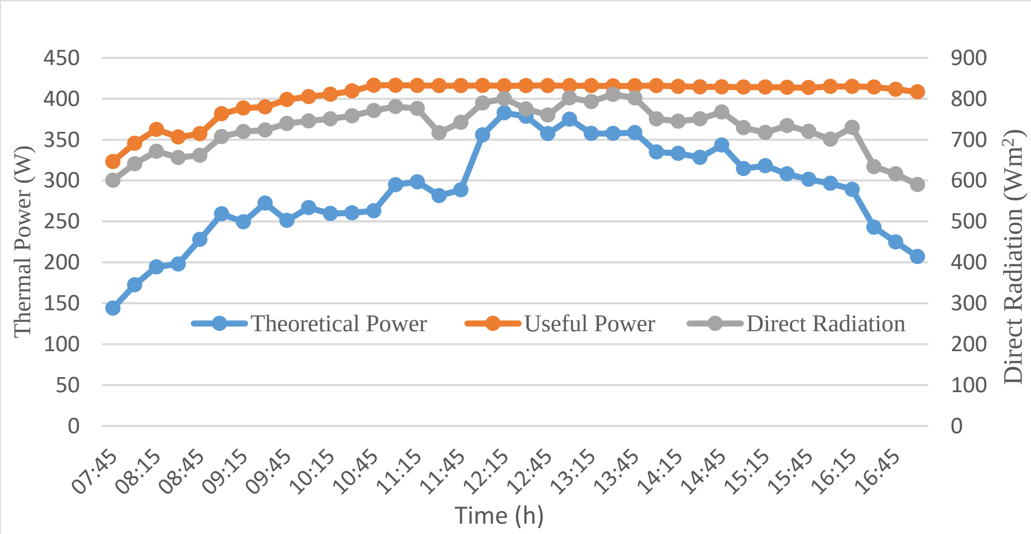


**Figure 5.** Theoretical and experimental thermal power and direct radiation values

Although the glass pipe temperature varies slightly in the experimental measurements in the collector, it is seen that the ambient, water inlet and outlet temperatures are in harmony (Figure 6). Since the parabolic is of small size, the difference between the inlet and outlet temperatures of the water is very small (Table 2).

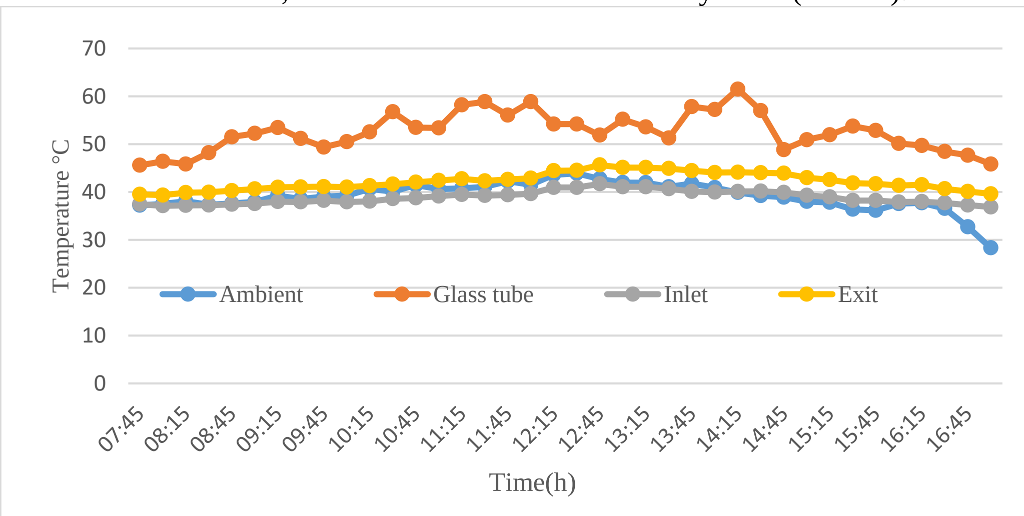


**Figure 6.** Ambient, glass pipe, water inlet, and outlet temperatures were measured in the parabolic collector

**Table 2.** Ambient, water inlet, and outlet temperatures were measured in the parabolic collector

| Ambient °C | Water Inlet °C | Water Outlet °C |
|---|---|---|
| 37,2 | 37,4 | 39,5 |
| 37,5 | 37,1 | 39,3 |
| 38,1 | 37,2 | 39,8 |
| 37,3 | 37,2 | 39,9 |
| 37,6 | 37,4 | 40,3 |
| 37,9 | 37,6 | 40,6 |
| 39,2 | 38,0 | 41,0 |
| 38,5 | 37,9 | 41,0 |
| 39,0 | 38,2 | 41,1 |
| 39,2 | 37,9 | 41,0 |
| 40,6 | 38,0 | 41,3 |
| 40,1 | 38,6 | 41,6 |
| 41,4 | 38,7 | 42,0 |
| 40,6 | 39,1 | 42,4 |
| 40,7 | 39,5 | 42,7 |
| 41,1 | 39,2 | 42,3 |
| 42,2 | 39,4 | 42,6 |
| 41,5 | 39,6 | 42,9 |
| 43,6 | 40,9 | 44,4 |
| 43,9 | 40,9 | 44,5 |
| 42,7 | 41,7 | 45,6 |
| 42,0 | 41,1 | 45,1 |
| 41,9 | 41,1 | 45,1 |
| 41,1 | 40,7 | 44,9 |
| 41,7 | 40,1 | 44,4 |
| 40,9 | 40,0 | 44,1 |
| 39,9 | 40,1 | 44,1 |
| 39,2 | 40,2 | 44,0 |
| 38,9 | 39,9 | 43,9 |
| 38,0 | 39,3 | 43,0 |
| 37,8 | 39,0 | 42,6 |
| 36,4 | 38,2 | 41,9 |
| 36,2 | 38,2 | 41,7 |
| 37,6 | 37,9 | 41,4 |
| 37,7 | 38,0 | 41,5 |
| 36,5 | 37,7 | 40,7 |
| 32,7 | 37,3 | 40,1 |
| 28,3 | 36,9 | 39,6 |

Figure 7 shows the graph obtained by direct radiation division of the thermal data and the inlet and ambient temperature values of the water. In this graph, the line equation for thermal efficiency shows a decreasing slope. Although the efficiency of the system is low, it is seen that it complies with the ASHRAE 93-863 standard for thermal applications [12,13,14,15].

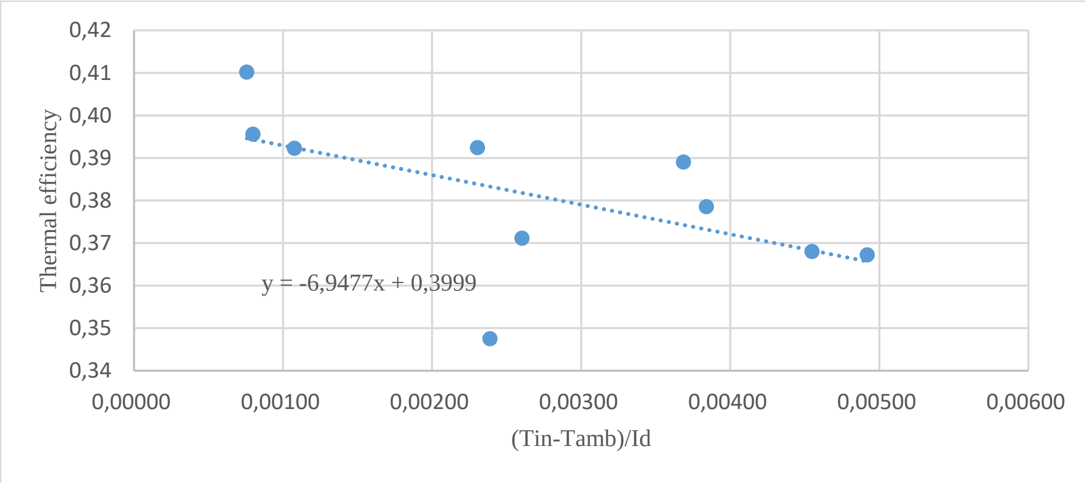


**Figure 7.** Thermal efficiency of the collector for hot water

## 6. Conclusions and Suggestions

If this collector, which is made in small sizes, can be made in larger sizes, more thermal power and high temperature can be obtained. The reason for choosing the reflective surface chrome-nickel material is that there is no ready-made mirror with a suitable parabola surface in the market. If a reflective mirror could be used, the thermal efficiency, power, and temperature would be greater. The theoretical and experimental values were close to each other. A thermal power of 380 W could be obtained from this collector with a collector area of 1.2 $m^2$ at noon. The thermal efficiency was the highest at 43% and the lowest at 26%.

## Conflict of Interest Statement

There is no conflict of interest between the authors.

## Statement of Research and Publication Ethics

The study is complied with research and publication ethics.

## Symbols

$A_a$ : Reflective surface area ($m^2$)

$A_y$ : Absorber surface area ($m^2$)

$C_p$ : Specific heat (kJ/kgK)

Id : Direct radiation ($W/m^2$)

$\dot{m}$ : Fluid flow rate (kg/s)

$T_{in}$ : Water inlet temperature °C

$T_{out}$ : Water outlet temperature °C

$T_a$ : Ambient temperature °C

$U_T$ : Total heat transfer coefficient ($W/m^2K$)

$Q_u$ : Useful energy (W)

$\gamma$ : Intercept factor (0.95)

: Collector thermal efficiency

$\tau$ : Heat transition coefficient (0.78)

$\alpha$ : Absorbtion coefficient (0.82)

$\rho$ : Reflection ratio (0.83)

## References

[1] A.Z, Hafez and et al., Design analysis of solar parabolic trough thermal collectors. *Renewable and Sustainable Energy Reviews* 82, pp. 1215–1260, 2018

[2] A. Kalogirou Soteris, *Solar Energy Engineering Processes and Systems*, Second Edition, printed Elsevier, 2014

[ 3] E. Venegas-Reyes et al., Design, construction, and testing of a parabolic trough solar concentrator for hot water and low enthalpy steam generation, *Journal of Renewable and Sustainable Energy* 4, pp.053-103, 2012

[4] E.A Irving Eleazar and et al., Design and Construction of a Parabolic Trough Solar Collector for Process Heat Production, *Energy Procedia* 57, pp. 2149-2158, 2014.

[5] G.K Manikandan and et al., Enhancing the optical and thermal efficiency of a parabolic trough collector-A review, *Applied Energy*, 235, pp.1524-1540, 2019.

[6] K.D Ramesh and K. Suresh, Thermal performance of parabolic trough collector with absorber tube misalignment and slope error, *Solar Energy*, 184, pp. 249-259, 2019.

[7] J.A Duffie and W.A. Beckman, *Solar Energy Thermal Processes*, John Wiley and Sons, New York 1991.

[8] A. Kılıç, Solar Energy, Kipaş Yayıncılık ,1984.

[9] F.P Incropera and D.P, DeWitt, *Heat and Mass Transfer*, Literatur Publishing (translation), Istanbul 2001.

[10] J.S., Hesieh, *Solar Energy Engineering*, Prentice-Hall,1986.

[11] H.Bulut, and et al, Measurement of Global Direct Beam and Diffuse Solar Radiation for Determining the Potential of Solar Energy Application, *State-University-Industry Cooperation Symposium and Marble Works Counci*l, 24-26 January, Diyarbakır, pp.484-490, 2010

[12] P.L Singh, R.M Sarviya and J.L Bhagoria, Thermal performance of linear Fresnel reflecting solar concentrator with trapezoidal cavity absorbers, *Applied Energy*, 87, pp.541-550, 2010.

[13] H.B Kulkarni, Design, and development of prototype cylindrical parabolic solar collector for water heating application, *International Journal of Renewable Energy Development*, pp.49-55, 2016.

[14] J.K Nayak, E.Y Amer and S.M Deshpande, Comparison of three transient methods for testing solar flat-plate collector, *Energy Conversions & Management*, 4, pp.677-700, 2000.

[15] E. Y, Amer, J. K Nayak and G.K Sarma, Transient test method for flat-plate collector: review and experimental evaluation, *Solar Energy*, 60 (5) , pp.229-243, 1997.